The Permeability Enhancing Mechanism of DMSO in Ceramide Bilayers Simulated by Molecular Dynamics

Rebecca Notman,* Wouter K. den Otter,† Massimo G. Noro,‡ W. J. Briels,† and Jamshed Anwar§

*Molecular Biophysics, Division of Pharmaceutical Science, King's College London, London, United Kingdom; †Computational Biophysics, University of Twente, Enschede, The Netherlands; ‡Physical and Chemical Insights Group, Unilever Research and Development, Port Sunlight, United Kingdom; and §Computational Laboratory, Institute of Pharmaceutical Innovation, University of Bradford, Bradford, United Kingdom

ABSTRACT The lipids of the topmost layer of the skin, the stratum corneum, represent the primary barrier to molecules penetrating the skin. One approach to overcoming this barrier for the purpose of delivery of active molecules into or via the skin is to employ chemical permeability enhancers, such as dimethylsulfoxide (DMSO). How these molecules exert their effect at the molecular level is not understood. We have investigated the interaction of DMSO with gel-phase bilayers of ceramide 2, the predominant lipid in the stratum corneum, by means of molecular dynamics simulations. The simulations satisfactorily reproduce the phase behavior and the known structural parameters of ceramide 2 bilayers in water. The effect of DMSO on the gel-phase bilayers was investigated at various concentrations over the range 0.0−0.6 mol fraction DMSO. The DMSO molecules accumulate in the headgroup region and weaken the lateral forces between the ceramides. At high concentrations of DMSO ($\geq$0.4 mol fraction), the ceramide bilayers undergo a phase transition from the gel phase to the liquid crystalline phase. The liquid-crystalline phase of ceramides is expected to be markedly more permeable to solutes than the gel phase. The results are consistent with the experimental evidence that high concentrations of DMSO fluidize the stratum corneum lipids and enhance permeability.

INTRODUCTION

The lipids of the topmost layer of the skin, the stratum corneum, constitute the main barrier to penetration of exogenous substances through the skin (1,2). Delivery of active molecules into or via the skin (transdermal delivery) can offer significant advantages over the more conventional routes of delivery, including the avoidance of the hepatic first-pass effects, less variability, better control, immediate termination of action if required, and improved customer/patient compliance (3). This promise, however, remains essentially unrealized, because for many molecules the skin constitutes a significant barrier. One approach to overcoming this barrier is to use chemical penetration enhancers such as dimethylsulfoxide (DMSO, $(CH_3)_2SO$) that interact with the skin lipids to facilitate the transport of active molecules across membranes (4). How such molecules increase the skin permeability is essentially still a mystery, but a greater understanding of their mechanism of action in this respect would be invaluable for the rational design of molecules that modulate the transport of active molecules in membranes. Molecules that decrease the permeability of membranes (or skin) are also of considerable interest for their potential ability to block absorption of toxic chemicals such as insect repellents, and pesticides and herbicides. Using molecular dynamics simulations, we have investigated the interaction of DMSO with gel-phase bilayers of ceramide 2, which is the predominant component of the stratum corneum lipids. High concentrations of DMSO have been found to induce a transition in the ceramide 2 bilayers from the ordered, tightly packed gel phase (the characteristic phase of skin lipids at body temperature) to the disordered, loosely packed liquid-crystalline phase. We propose this phase transformation as one possible mechanism by which DMSO enhances permeability.

The stratum corneum consists of dead cells known as corneocytes embedded in an intercellular matrix of lipids in a ''bricks and mortar'' type arrangement (1,5). The lipids consist mainly of ceramides (~50%), cholesterol (~25%), cholesterol sulfate (~5%), fatty acids (10–15%), and a small amount of cholesterol esters, with little or no phospholipids (6). Together, the stratum corneum lipids form lamellar structures that are considered to exist either as bilayers or as three-layer sandwich-type structures comprising a softer, more fluid inner layer surrounded by condensed outer layers (7). The phases are essentially crystalline, with the lateral packing of the alkyl chains being orthorhombic, though some looser-packed hexagonal gel phase confined to the topmost layers of the stratum corneum has also been observed (8–11).

The ceramide lipids, a conserved feature of eukaryotic cells, are rather ubiquitous. At the cellular level they play a key functional role as signal transducers, involved in the regulation of cell proliferation and differentiation and in apoptosis (12–14). Within the skin, the ceramides play a pivotal role in the skin's barrier function. The skin lipids contain at least nine different types of ceramides, comprising

Submitted January 24, 2007, and accepted for publication May 15, 2007.

Address reprint requests to Jamshed Anwar, Computational Laboratory, Institute of Pharmaceutical Innovation, University of Bradford, Bradford, UK. E-mail: j.anwar@bradford.ac.uk.

Editor: Peter Tieleman.

0006-3495/07/09/2056/13 $2.00

doi: 10.1529/biophysj.107.104703

a base, which can be a sphingosine, a phytosphingosine, or 6-hydroxysphingosine (all with chain length C16), linked to a nonhydroxy or α-hydroxy fatty acid of varying alkyl chain length. At skin temperature ($\sim$305 K) the pure ceramides exist in the ordered gel phase (15,16). They form a network of hydrogen bonds in the plane of the bilayer, and, in the anhydrous state, also across the lamellar layers (17–19). Together, these properties are considered to confer rigidity and structural integrity to the stratum corneum, contributing to the highly impermeable nature of skin. The most abundant of the ceramides in the stratum corneum lipids is ceramide 2 (see Fig. 1), which is based on sphingosine. Its fatty acid chain length varies, with the most common chain length being C24. The presence of asymmetric ceramide molecules in lipid bilayers has been shown to affect membrane organization (20). Ceramide 2 is relatively well characterized in terms of its physical and thermodynamic properties (15,21–26). In the bilayer gel phase, it can exist in two distinct forms, namely orthorhombic or hexagonal, that differ in terms of the packing of the hydrocarbon chains. At $\sim$353$-$363 K it undergoes a transition to a disordered phase (15,22). Whether the disordered phase is a liquid-crystalline phase or a nonbilayer phase such as an inverted hexagonal phase is still not clear. Ceramide 2, a sphingosine ceramide, forms a more tightly packed arrangement than its phytosphingosine analogs (23,27). In the anhydrous orthorhombic phase and the hexagonal gel phase, ceramide 2 tends to form intermolecular hydrogen bonds across the lamellar layers rather than in the plane of the bilayer (18).

Many compounds are known to compromise the barrier function of the skin and to facilitate the penetration of active molecules. These include urea and its derivatives, alkyl sulfoxides including dimethylsulfoxide (DMSO), various surfactants, oleic acid, and Azone (1-dodecylazacycloheptan-2-one or laurocapram) (4,28–31). The effects of DMSO are concentration-dependent, and it is reported that concentrations in the region of 60% in the formulation are required to achieve significant enhancement (4). (It is not clear from the literature what the units are for the stated concentration; the 60% value in percent w/w terms equates to 0.26 mol fraction DMSO). DMSO is found to be effective for both hydrophilic and hydrophobic molecules. Although the penetration enhancement effects of DMSO have been investigated extensively, an accurate molecular-level description of its mode of action (or, for that matter, that of any other known penetration enhancer) is still lacking. The interaction of DMSO with lipids is thought to be important in its enhancing action. It has been proposed that DMSO promotes lipid fluidity by disrupting the ordered structure of the lipid chains, which enhances the diffusion of solutes. Differential scanning calorimetry experiments on human skin show that DMSO lowers the temperature of the two phase transitions associated with lipid chain melting (32). In addition, Fourier transform Raman spectroscopy on DMSO-treated human skin suggests that DMSO at high concentrations disorders the lipid chains of the stratum corneum (33). It has also been suggested that DMSO may interact with membrane proteins, leading to structural defects at the protein-lipid interface, which may enhance permeability (DMSO readily denatures proteins and is known to alter the conformation of the intercellular keratin in the stratum corneum) (34).

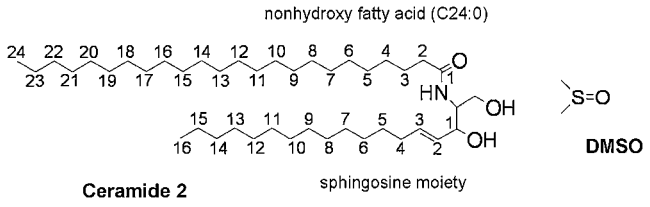

FIGURE 1 Molecular structure of ceramide 2 and DMSO. Carbon atom numbering corresponds to that given for the lipid-tail-order parameters.

DMSO is also known to interact strongly with phospholipids, and is widely employed in cell biology for its ability to induce cell fusion and differentiation, and as a cryoprotectant (35–38). Again, the molecular basis for these actions is lacking, but important insights have been gained from molecular simulation (39–41). Molecular dynamics simulations of DMSO-dipalmitoylphosphatidylcholine (DPPC) systems using a coarse-grained model reveal that DMSO modulates the mechanical properties of the bilayer, reducing both the area compressibility and bending moduli and hence making the membrane more floppy (41). A floppier membrane will facilitate membrane fusion processes and help accommodate mechanical stresses resulting from ice formation during cryopreservation. The simulations also reveal that at high concentrations DMSO can induce water pores into the bilayer, which may be an important mechanism for permeability enhancement of solutes.

In contrast to phospholipids, molecular simulation of skin lipids remains essentially an unexplored niche. Notable studies include simulations of a stratum corneum lipid model consisting of a fatty acid and cholesterol (42), ceramide channels embedded in a phospholipid bilayer (43), and a 16:0 ceramide 2 bilayer in the liquid-crystalline phase (44). To the best of our knowledge, no simulations of stratum corneum lipids in the gel phase—which is the most relevant phase of the skin lipids under physiological conditions—have yet been reported. Simulations of the bilayer gel phase are particularly challenging, as the dynamics are much slower compared to the commonly simulated fluid phase bilayers. We note that although it may be tempting to investigate heterogeneous systems that relate more closely to the stratum corneum lipid composition, it is important, in the first instance, to characterize and understand the behavior of the key component of skin lipids, namely the ceramides. In this spirit, we report here, in atomistic detail, molecular dynamics simulations of pure ceramide bilayers in water in both the gel and liquid-crystalline phases, and in a range of concentrations of DMSO in the gel phase.

SIMULATION METHODOLOGY

Molecular dynamics simulations were performed on bilayer systems of pure ceramide 2 in water at 283 K, 323 K, and 363 K and ambient pressure. It was anticipated that simulations at these temperatures would yield ceramide bilayers in the phases that are observed experimentally (orthorhombic/crystalline packing, hexagonal/gel phase, and possibly a liquid-crystalline phase). As the phase diagram of the current potential model of ceramide 2 has not yet been established, we opted for the ''mid-range'' temperature of 323 K instead of skin temperature (~305 K). The systems comprised 128 ceramide molecules arranged in a bilayer structure (64 molecules/leaflet) surrounded by water. The lipid/water molecule ratio was 1:40.

The simulation of a gel-phase structure can present major technical challenges because of ergodicity problems. As the dynamics of such systems are relatively slow, the ''equilibrated'' structure is likely to be not too dissimilar to the starting configuration. The starting configuration could be based on a crystalline structure, assuming it is known and that the molecules exhibit bilayer packing, or it could be an inspired guess. An alternative approach is to first equilibrate the system in the fluid phase and then to either cool or pressurize it to induce the transition to the gel phase. Each of these approaches has drawbacks. Although direct simulation of the solid state could lead to kinetic trapping, cooling a fluid phase over simulation timescales is akin to quenching, which could lead to supercooling rather than the required transition to the gel phase. We adopted both the direct approach, i.e., simulation of the solid phase starting from an idealized structure, and also cooling an equilibrated fluid phase. In generating the starting bilayer configuration, we laterally replicated a pair of ceramide molecules in the hairpin conformation with their hydrocarbon tails facing each other to yield a bilayer patch with the molecules sitting on an orthorhombic lattice. Two distinct starting configurations were considered for the molecule pairing: 1), a partially interdigitated configuration where the short tail of one molecule was packed end-to-end with the long chain of the opposite molecule; and 2), a noninterdigitated configuration in which the long chains (and the short chains) were in line with each other. For the direct approach, the lattice bilayer structures were immersed in water and equilibrated at 323 K. For generating the fluid phase, we employed positional restraints (which were gradually weakened) on the terminal particles of the lipid tails in a bid to get the system to adopt the traditional bilayer structure characteristic of phospholipids, with all of the lipid molecules in the hairpin conformation. The equilibrated fluid bilayer was then cooled by dropping the temperature stepwise. For all the procedures, the resulting gel structures were very similar, with tails packed hexagonally and a tail interdigitation somewhere between nonexistent and partial. Another characteristic feature was that some of the lipid tails extended into the interface region, which also occurred in the fluid phase. These observations are discussed in detail in the next section. The equilibrated bilayer patch, whose original configuration comprised interdigitated molecules, was used as the starting configuration for the studies presented here.

Molecular dynamics simulations were also carried out on ceramide bilayers in the gel phase at 323 K in 0.1, 0.2, 0.3, 0.4, 0.5, and 0.6 mol fraction DMSO with respect to the solvent water. The compositions of the various systems are given in Table 1. In the initial configurations, the DMSO molecules were located randomly within the water region.

The potential function and interaction parameters employed for the ceramide were based on the united atom force field of Berger (45), which is parameterized for phospholipids and uses GROMOS87 parameters for headgroups and specially adapted parameters for lipid tails. This force field has also been used in simulations of palmitoylsphingomyelin (46) that has a similar molecular structure to ceramide 2 except for a phosphatidylcholine headgroup. The atomic partial charges for the ceramide headgroup were taken from the side chain of serine (ceramide backbone of palmitoylsphingomyelin) in the manner of Mombelli and co-workers (46). The atoms were partitioned into small neutral charge groups to reduce discontinuities in the potential at the interaction cutoff. The united atom carbons in the lipid tails had a partial charge of zero. The water model was simple point charge (47) and the DMSO model was that of Bordat (48).

TABLE 1 Composition of simulated bilayer systems

DMSO* (mol fraction)	No. of H_2O molecules	No. of DMSO molecules	Temperature (K)
0	5120	0	283, 323, 363
0.1	4608	512	323
0.2	4096	1024	323
0.3	3584	1536	323
0.4	3072	2048	323
0.5	2560	2560	323
0.6	2048	3072	323

Systems contained 128 ceramide molecules each.
*DMSO values given are with respect to water.

The simulations were carried out in the NPT ensemble using the Gromacs package (49), and employed the Berendsen thermostat and an anisotropic pressure coupling with the simulation cell kept orthogonal. The effect of using a full anisotropic pressure coupling (i.e., where the three box dimensions and angles are free to equilibrate independently of one another) was also examined. Throughout these latter simulations, the system box remained essentially orthogonal to within 0.5° and system properties were identical to those for the semianisotropic pressure coupling. All bonds in the system were constrained using the SHAKE algorithm (50). The time step was 2 fs and the interaction cutoff for both the Lennard-Jones and Coulombic interactions was 1.2 nm. The use of Ewald summation for the electrostatics was investigated but was not found to yield any significant structural differences from simulations where the electrostatics were truncated. Consequently, for computational efficiency we proceeded with truncation of the electrostatics. We are aware that in atomistic simulations of phospholipids, it has been argued that the use of a cutoff for the electrostatic interactions introduces some structural artifacts (51). The apparent inconsistency with the work of Patra et al. (51) probably results from the fact that in contrast to phospholipids, ceramides do not contain any atoms with full formal charges and the small charge groups were specifically designed to be neutral (52). Equilibration time was typically 5 ns but was extended up to 20 ns for the systems containing ≥0.4 mol fraction DMSO to enable the area/lipid in these systems to reach its equilibrium value. Equilibrium properties were averaged over 15 ns.

RESULTS AND ANALYSIS

Pure ceramide bilayers

Before studying the effects of DMSO on a ceramide 2 bilayer, we first characterize the membrane in a purely aqueous solvent.

Phase behavior

Experimentally, ceramide 2 exhibits the gel-to-liquid-crystalline phase transition over the temperature range 353–363 K. The gel phase itself exhibits two variant structures, namely an orthorhombic phase below ~333 K, and a hexagonal phase above 333 K (15,53). Although it might be good practice to explore the full phase diagram, it is simply not efficient to carry out molecular dynamics simulations at an extended series of temperatures. We have carried out simulations at 283 K, 323 K, and 363 K, with the expectation that these temperatures would select each of the relevant bilayer phases of ceramide 2. Over the timescale of the simulations, the area/lipid converges to a constant value as

shown in Fig. 2, indicating that the bilayers have reached equilibrium configurations. At the lower temperatures, 283 K and 323 K, the simulations reveal gel-phase structures with the lipid tails in a hexagonal arrangement (see Fig. 3). There was no hint of orthorhombic chain packing even at 283 K, but this may not be a limitation of the molecular model. The gel-phase structure is essentially a solid in which the processes occur over a long timescale, and it may be that the energy barrier for the hexagonal-orthorhombic transition is rather high, making the transition an improbable event in a simulation. A snapshot of the ceramide bilayer at 323 K is shown in Fig. 4. It is apparent, at least for the left leaflet, that the lipids are packed in the gel phase with the tails aligned at a slight angle (~17°) to the bilayer normal. The packing is also ordered for the right leaflet, though this is not clear from the figure because the orientation of these packed lipid tails is not in phase with that of the left leaflet. Due to the mismatch in the length of the two hydrocarbon chains of the ceramide, the lipids are not so tightly packed at the center of the bilayer, where the packing is almost characteristic of the liquid-crystalline phase rather than the gel phase. At the higher temperature of 363 K the bilayer undergoes a transition to the liquid crystalline phase and the lipid tails no longer show any order in their packing (Fig. 3).

Ceramide molecule conformation

The ceramide bilayers show some unexpected features, including the presence of ceramide tails straddling the interface and the seemingly loose packing of the ceramide headgroups to the extent that there appear to be large spaces between adjacent ceramide headgroups. These hitherto unobserved structural features stem from the conformational flexibility of the ceramide molecule coupled with the asymmetry of the chain lengths. Some of the various conformations adopted by ceramide molecules in the bilayers are shown in Fig. 5. Many of the molecules adopt the expected hairpin conformation, as shown in Fig. 5, *a* and *b*, and integrate into the bilayer leaflets

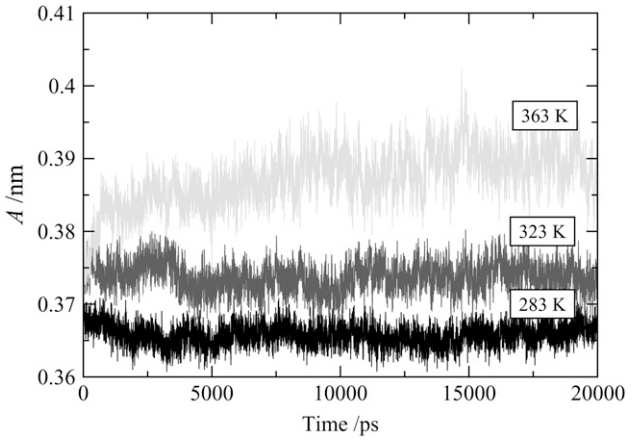

FIGURE 2 Area/lipid of the pure ceramide bilayers at different temperatures as a function of time.

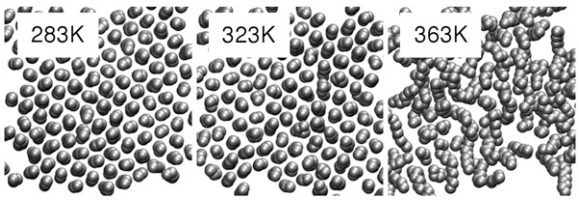

FIGURE 3 Cross section perpendicular to the bilayer normal of the hydrocarbon chains in one of the monolayers of the pure ceramide bilayer systems. At 283 K and 323 K, the lipid tails pack in a hexagonal arrangement, whereas at 363 K the packing of the tails is liquid-like.

in the usual manner, i.e., the headgroups are in contact with the water, whereas the tails align into the hydrophobic region. It is clear from Fig. 5, *a* and *b*, however, that the asymmetry of the tail lengths makes the packing of the tails challenging and the molecules struggle to accommodate the extended part of the C24 chain. Although from a two-dimensional representation of the ceramide 2 molecule it would seem that these molecules could pack perfectly into a bilayer by partial interdigitation, the simulations reveal that this is not feasible to any significant extent. An approach adopted by the lipids for dealing with the incommensurability of the asymmetric tails is to retract the extended C24 chain, bringing some of the alkyl groups into the interface region, and to present a more symmetric set of tails at the bilayer core, as shown in Fig. 5 *d*. A variation on this approach appears to be to straddle over a nearest neighbor, which again enables the molecule to accommodate some of the alkyl groups at the interface region and to pack its tails optimally at the core of the bilayer, as shown in Fig. 5, *c* and *e*. Yet another approach, which appears to be rather drastic, is for the molecule to present only a single tail into the hydrophobic region, with the other tail lying tangentially to the bilayer at the water-lipid interface (Fig. 5 *f*). This remarkable feature of tails sticking out of the bilayer is fully reproducible and has been observed for a number of distinct starting conformations. It even occurs when weak restraints are imposed on the terminal tail atoms to encourage them to remain in the center of the bilayer. As will be discussed below, the tails

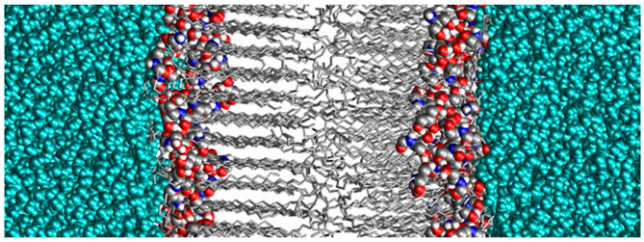

FIGURE 4 Snapshot of the ceramide bilayer in the gel phase at 323 K. The ceramide tails of both layers are packed in a hexagonal arrangement, although this is not apparent for the right leaflet because of a difference in orientation. The *z* axis runs in a direction normal to the bilayer surface. Water is cyan, ceramide carbon atoms gray, nitrogen atoms blue, oxygen atoms red, and hydrogen atoms white.

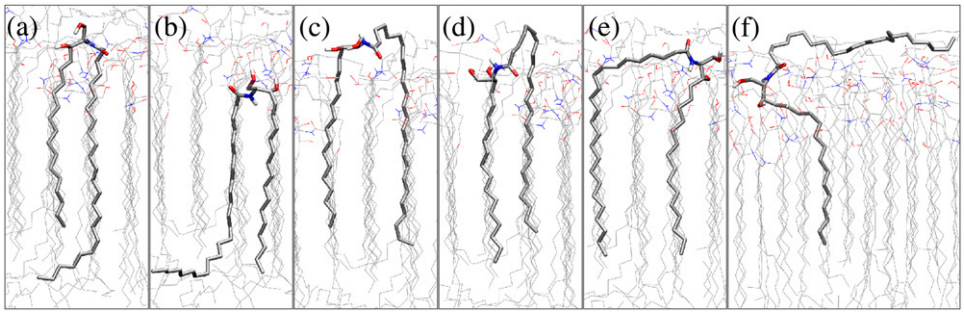

FIGURE 5 Snapshots from the simulation of the bilayer at 283 K showing examples of the different conformations adopted by the ceramide molecules in the bilayer. Carbon atoms are gray, nitrogen atoms blue, oxygen atoms red, and hydrogen atoms white.

reinsert back into the bilayer interior when a small fraction of DMSO is added to the solvent, to resurface again after the removal of this fraction. The picture that emerges is that the ceramide molecule has considerable conformational flexibility that it exploits in dealing with the packing of the asymmetric tails. It appears that the molecules readily pay the penalty of exposing some alkyl groups at the water-lipid interface in a bid to reduce tail-end mismatch at the hydrophobic core. The penalty (in terms of both energy and entropy) for presenting an entire lipid tail at the water-lipid interface is expected to be rather high in most lipid bilayers, and on this basis one might assume that such a configuration would be relatively improbable. A possible explanation is that the penalty may not be as high as perceived due to the relatively low hydrophobic shielding provided by the small headgroups of the ceramides (see below). The resulting high density of alkyl groups near the water-lipid interface may make this interface region a relatively agreeable environment for lipid tails attempting to minimize the packing incommensurability at the bilayer core. The high alkyl density makes the water-lipid interface sharp and hydrophobic, and explains why the tail order-parameter profiles show greater disorder close to the interface (see below), as well as the existence of the small peak at the interface observed in the density profile of the tail groups (see below). It is pertinent to note that when these same force-field parameters are used to simulate C16:0 ceramide 2 bilayers (where the tails are of equal length), the ceramide molecules retain their hairpin conformation and show little if any inclination of exposing their tails into the aqueous region (C. Das and M. G. Noro, Unilever Research & Development, Port Sunlight, UK, personal communication, November 2006).

Area/lipid

As for the packing of the headgroups of the ceramide, the headgroups appear to be loosely packed and disordered, with significant gaps between them at all temperatures. We assume this to be due to the small size of the headgroup relative to the exclusion area of the alkyl chains. Water molecules bridge many of these headgroups, but we also observe that the gaps between headgroups are sometimes filled with the ceramide tails. This point was discussed above. The projected area/lipid, A, for each temperature, is given in Table 2. As expected, the area/lipid increases with temperature as the thermal energy causes increasing loosening of the tail packing. The area/lipid for the gel phase at 323 K is 0.374 nm^2, which is close to the known experimental values of 0.378 nm^2 (27) and 0.4 nm^2 (26) determined from surface-pressure isotherms of C16:0 ceramide 2 monolayers. There appear to be no experimental data for the liquid-crystalline phase, nor for bilayers of the C24:0 ceramide 2. Our area/lipid values are very close to those obtained for C16:0 from molecular dynamics simulations by Das and Noro (C. Das and M. G. Noro, Unilever Research & Development, Port Sunlight, UK, personal communication, November 2006), who also used the same forcefield. There is, however, some disparity with respect to the value for C16:0 obtained from a simulation by Pandit and Scott (44); the present simulations of C24:0 yield 0.388 nm^2 at 363 K, whereas Pandit and Scott's value for C16:0 was 0.55 nm^2 at 368 K.

Density profiles

The density profiles of the gel phase at 283 and 323 K and the liquid-crystalline phase at 363 K are shown in Fig. 6. In general terms, the profiles are rather similar for all three bilayers. Going from left to right, we first pass a flat region corresponding to bulk water. There is then a decrease in the density at the interface, where the water interacts with the headgroups. Closer to the center of the bilayer, the total density peaks in the region where the headgroups lie. Next, the local density in the region of the closely packed ceramide alkyl chains is comparable to that of the bulk water, and finally one observes a low density in the center of the bilayer, corresponding to the loose random packing of the tail ends. It is noteworthy that there is a shoulder (with a minor peak on one of the leaflets) in tail-group density in the region of the interfaces. These shoulders correspond to some of the alkyl chains actually lying parallel to the lipid-water interface. This phenomenon, which was discussed earlier, occurs in each of the bilayers, regardless of temperature. In the liquid-crystalline phase, the lipid tails are disordered, resulting in a less dense structure. The larger peak in the tail-density distribution at the interface reveals that the number of ceramide tails lying parallel to the lipid-water interface increases relative to the gel phase. This results in a broadening of the bilayer-water interface compared with the gel phase.

TABLE 2 Area/lipid, interfacial width, bilayer thickness, and area compressibility modulus of pure ceramide bilayer systems at different temperatures

T (K)	A (nm^2)	Interfacial width (nm)	Bilayer thickness (nm)	K_A (mN m^{-1})
283	0.366 (±0.001)	0.42	4.88	12000 (±1000)
323	0.374 (±0.002)	0.54	4.94	7900 (±700)
363	0.388 (±0.005)	0.62	4.95	1530 (±80)

T, temperature; A, area/lipid; K_A, area compressibililty modulus.

Bilayer thickness

The width of the ceramide/water interface can be estimated as the distance over which the water density rises from 10 to 90% of the bulk value and is given in Table 2. The interface region is extremely narrow (~0.4–0.6 nm) compared with, for example, sphingomyelin bilayers which have an interfacial thickness of ~1 nm (46). Unlike sphingomyelin, ceramide headgroups are very small and they will probably only be surrounded by a small solvation shell. This sharp interface, which indicates that almost no water penetrates the bilayer, is consistent with the accepted view that ceramides are responsible for the relatively low water permeability of the stratum corneum. As the temperature is increased, more ceramide tails protrude into the interface region, which effectively increases the width of the interface. The bilayer thickness, estimated from the peaks of the headgroup distribution, is given in Table 2. At all temperatures, the bilayer thickness is smaller than the total length of two ceramide molecules, which indicates that there is a degree of interdigitation of the tails. The thickness (~4.9 nm) is comparable to that estimated for the partially interdigitated crystal structure of ceramide in the hairpin conformation, namely 5.2 nm (54). The bilayer thickness increases slightly with temperature, which may be due to the expansion of the hydrocarbon region of the bilayer.

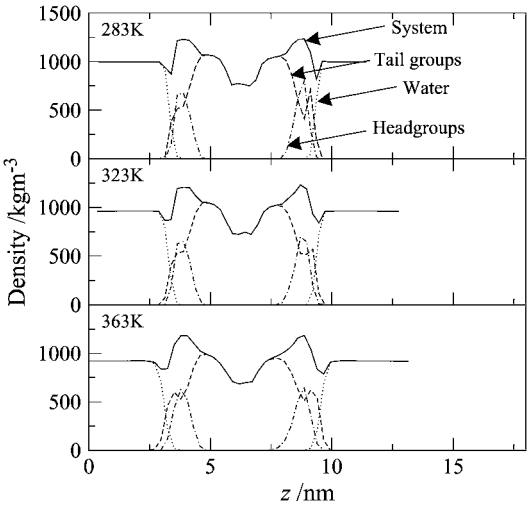

FIGURE 6 Density profiles of the various components and moieties of the pure ceramide bilayer at 283, 323, and 363 K.

Lipid tail order

Lipid-tail-order parameters provide a measure of the alignment of the hydrocarbon chains in the bilayer. The order parameter S_z for atom C_n was calculated using $S_z = 3/2(\cos^2\theta_z) - 1/2$, where θ_z is the angle between the z axis (the normal to the bilayer) of the simulation box and the vector C_{n-1} to C_{n+1}. The order parameters of atoms in each chain are shown in Fig. 7. The order parameter profiles for all the bilayers are qualitatively similar, with a lower overall ordering of the C24 chain relative to the C16 chain. There appears to be a higher degree of disorder in both chains for alkyl groups close to the interface, which in particular for the C24 chain is mainly due to the loops depicted in Fig. 5, *c–e*. The order of the tails then increases going down the chain and decreases again toward the center of the bilayer. We expect the chains to become more disordered in the center, where they have a greater degree of conformational flexibility, particularly the C24 chains, which extend into the core region. The hydrocarbon chains of the system at 283 K are slightly more ordered than the chains of the system at 323 K because of the closer packing of the lipids at the lower temperature. At 363 K the hydrocarbon chains of the system are significantly more disordered than those at the lower temperatures. This increase in lipid tail disorder is consistent with the bilayer existing in the fluid phase at this temperature.

Hydrogen bonding

The cohesiveness of the skin barrier is often attributed, in part, to the lateral hydrogen-bonding network between the ceramide headgroups (18). Analysis of hydrogen bonding in the systems confirms that such a network indeed exists. The average numbers of ceramide-ceramide and ceramide-water hydrogen bonds per ceramide molecule were determined to be ~2.8 and 0.3, respectively, for the three systems. The

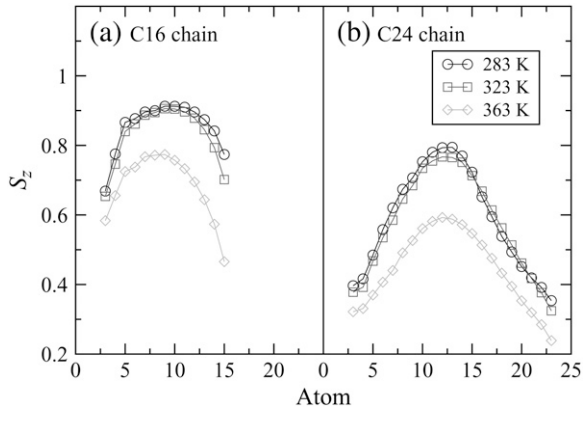

FIGURE 7 Lipid-tail-order parameters S_z that indicate the alignment of the chain as a function of carbon number (indicated in Fig. 1) of (*a*) the C16 chain and (*b*) the C24 chain of the ceramide bilayer at different temperatures.

hydrogen bonds were defined using the geometrical criterion that a hydrogen bond exists if the distance between the donor and acceptor atom is $\leq$0.35 nm and if the acceptor-donor-hydrogen angle is $\leq$60° (55). For the gel phase, each ceramide molecule on average forms about three hydrogen bonds with its neighboring ceramide molecules. Almost all of these ceramide-ceramide hydrogen bonds involve one or both of the two hydroxyl groups. We also find that the water molecules preferentially hydrogen-bond to the carboxyl oxygen of ceramide, and there is negligible hydrogen bonding between water and the two hydroxyl groups or the amide group of the ceramide headgroup. Likewise the ceramide molecules in the liquid-crystalline phase form about three hydrogen bonds with their neighbors, indicating that the interactions between ceramide headgroups are not disrupted in the liquid-crystalline phase.

Elasticity

The area compressibility modulus K_A, which is a measure of the elasticity of the membrane, was calculated from the variance in the fluctuations in the area/lipid for the equilibrated systems, $K_A = k_B T A_0/\langle \delta A^2 \rangle$, where A_0 is the equilibrium area/lipid, and is tabulated as a function of temperature in Table 2. The values obtained by this approach are possibly influenced by the choice of barostat and the strength of its coupling to the simulation cell (56); hence, an independent approach was used to verify these moduli for two systems, namely the pure ceramide bilayer at 323 K and the system containing 0.1 mol fraction DMSO at the same temperature. This alternative approach involved a series of constant surface-area (NAP_zT) simulations in which the surface tension γ was monitored as a function of the area/lipid. The surface tension is calculated as the difference between the components of the pressure tensor in the direction normal to the bilayer and those parallel to the bilayer, $\gamma = \langle L_z(P_{zz} - 0.5(P_{xx}+P_{yy}))\rangle$, where L_z is the length of the simulation box along the z axis. The area compressibility is then calculated by fitting $\gamma = K_A(A - A_0)/A_0$ to the stress-strain curve of the bilayer. The K_A values obtained in this way are shown in Fig. 8, and they show reasonable agreement. For the pure ceramide systems, the area compressibility modulus decreases with increasing temperature, indicating that the bilayer becomes more compressible with rise in temperature. In general and in absolute terms, the K_A values (Table 2) are an order higher than those of phospholipid bilayers in the gel phase, which are reported to have a compressibility modulus of $\sim 10^3$ mN m^{-1} (57) (values around 300 mN m^{-1} are more typical for the phospholipid liquid-crystalline phase). Our values are comparable to those reported for simulated liquid-crystalline sphingomyelin bilayers, namely 4.4×10^3 mN m^{-1} (58). The high compressibility modulus, which reflects a more rigid structure, is attributed to the extensive hydrogen-bonding network involving the headgroups.

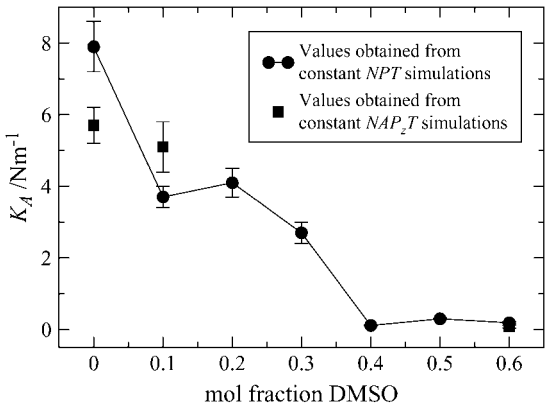

FIGURE 8 Area compressibility modulus K_A calculated from the fluctuations in the area of ceramide bilayers as a function of DMSO concentration (*circles*) and from constant-area simulations (*squares*). Error bars refer to the standard error.

Ceramide bilayers with DMSO

We now address the effects of DMSO on the properties of ceramide 2 bilayers at 323 K, with the objective of obtaining insights into the possible mechanism of action of DMSO as a penetration enhancer.

Phase behavior

Snapshots of the equilibrated pure ceramide bilayer and bilayers containing the different concentrations of DMSO are shown in Fig. 9. The lipids persist in the gel-phase structure, with hexagonally packed tails at all concentrations of DMSO up to 0.3 mol fraction. At 0.4 mol fraction DMSO, the bilayer transforms to a liquid-crystalline structure characterized by the disordered lipid tails and the onset of lateral diffusion of the lipids. The simultaneous reduction of the bilayer thickness suggests that the interdigitation of the lipids has increased. By visual inspection, we observe that DMSO molecules and the occasional water molecule start to penetrate into the membrane. The DMSO molecules in some instances form continuous chains through the bilayer, but no such chains are observed for the water molecules. At the

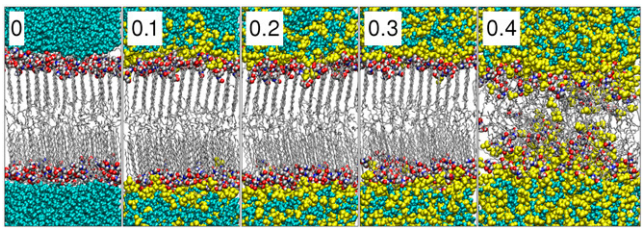

FIGURE 9 Snapshots of the ceramide bilayers with different concentrations (mol fraction with respect to the solvent) of DMSO. DMSO induces a transition from the gel to the liquid-crystalline phase at concentrations $\geq$0.4 mol fraction DMSO. Water is cyan, DMSO yellow, ceramide carbon atoms gray, nitrogen atoms blue, oxygen atoms red, and hydrogen atoms white.

highest concentrations of DMSO, the bilayer shows signs of losing its integrity in that there is a high degree of interdigitation and the interface is very diffuse, although the overall lateral structure is maintained during extended simulations.

Gel-phase simulations, because of the slow dynamics and kinetic trapping, are prone to ergodicity problems, with the implication that in some instances the simulations may not reach equilibrium. Convergence of appropriate system properties can be helpful indicators of a system approaching equilibrium, while reversibility of a transition could provide some confidence that equilibrium states are being sampled. However, these indicators are by no means infallible: system properties could show convergence for a system that becomes stuck in a metastable state, whereas inability to show reversibility over simulation timescales does not necessarily mean that the respective states are not equilibrium states. The gel-fluid phase transition is first order, and such transitions occur by activated processes, and kinetics in the forward direction need not be of the same magnitude as in the reverse direction. For molecules with extensive conformational flexibility, such as lipids, the ordering transition tends to be significantly slower than the disordering transition. Despite these reservations, we have examined the convergence of the area/lipid for each bilayer as a function of simulation time (see Fig. 10), which confirms that systems are equilibrated, and have also explored the reversibility of the gel-fluid transitions induced by DMSO. With respect to the latter, we looked at the reversibility of the gel-fluid transition induced by 0.4 mol fraction DMSO system. For this system, some of the DMSO was replaced by water to yield a bilayer with 0.3 mol fraction DMSO. After the removal of DMSO, we observed a sharp decrease in the area/lipid, which is consistent with the onset of the transition to the gel phase and a strong indication that the liquid crystalline phase is not stable at a 0.3 DMSO mol fraction. The slowly ordering system did not manage to fully recover the gel phase, nor did the area/lipid converge to a constant value, within the simulation timescales. We also explored the effect of dispersing 0.1 mol fraction DMSO throughout the gel phase bilayer, rather than placing it within the bulk water phase. In this simulation, the majority of the DMSO molecules rapidly diffused out of the bilayer toward the interface and into the aqueous phase. A small number of the molecules formed a cluster in the central region of the bilayer, where they may be kinetically trapped. The bilayer remains in the gel phase, confirming that this is the preferred state at 0.1 mol fraction DMSO.

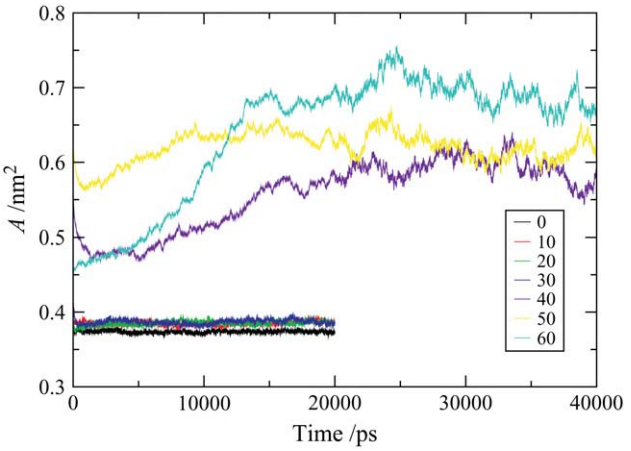

FIGURE 10 Area/lipid of the ceramide bilayer systems containing different concentrations of DMSO as a function of time.

Density profiles

The molecular densities of the molecules (and moieties) of ceramide 2, DMSO, and water as a function of the position along the bilayer normal (z axis) in the pure ceramide bilayer and bilayer systems containing DMSO are compared in Fig. 11. The plots can be grouped into two categories, those that correspond to the gel-phase structure (the pure system and systems containing 0.1−0.3 mol fraction DMSO), and those corresponding to the liquid-crystalline phase (0.4−0.6 mol fraction DMSO).

For bilayer systems containing low concentrations of DMSO, the density profile of ceramide does not differ significantly from that of the bilayer without DMSO, i.e., the gel-phase structure, indicating that the overall structure of the ceramide bilayers is unchanged in these systems. The water-density profiles reveal that the water-lipid interface shifts away from the bilayer surface as the concentration of DMSO increases. Viewing this in conjunction with the DMSO profile reveals that the water present at the interface (and

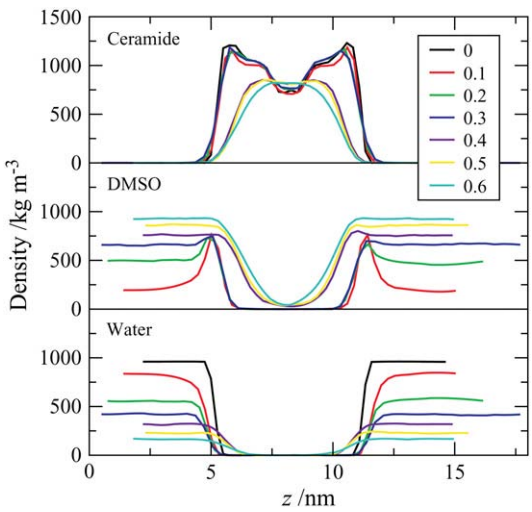

FIGURE 11 Density of ceramide, DMSO, and water as a function of the position z along the bilayer normal for the pure ceramide bilayer system and systems containing varying concentrations of DMSO. The z axis length of the simulation box was different for each of the systems due to different specific volumes of solvent mixtures and to pressure scaling. Consequently, to enhance clarity, the profiles have been shifted relative to each other so that the center of each bilayer is at the same position on the z axis of the plot.

interacting with ceramide headgroups) is replaced by DMSO. The DMSO density profiles also reveal an extraordinary tendency of DMSO to accumulate at the interface, as indicated by a large peak in the DMSO density in this region. The phenomenon is particularly visible at the low concentration of DMSO (0.1 mol fraction), for which the DMSO density profile shows a low density in the bulk but a significant peak at the interface. As the concentration of DMSO is increased, the peak density of the DMSO at the interface does not change; rather, the concentration of DMSO in the bulk solvent increases. This suggests that there is a saturation limit for DMSO at the interface, which is attained at low concentrations of DMSO in the solvent. The implication is that at low concentrations, any effects of DMSO are unlikely to show a dependence on concentration. The sharp hydrophobic interface of the ceramide gel phase presents an ideal environment for DMSO molecules, because they are small, amphiphilic, and capable of serving as hydrogen-bond acceptors.

Upon increasing the overall DMSO fraction, the resulting DMSO concentration in the solvent eventually matches that of the saturated interfacial layer at a mol fraction of ~0.4. The bilayer systems with ≥0.4 mol fraction DMSO differ significantly in their density profiles from the pure ceramide bilayer and the systems with low concentrations of DMSO. A noticeable reduction in the width of the ceramide density profiles, in combination with the vanishing of the low density region in the center of the bilayer, suggests that there is a greater degree of interdigitation of the ceramides. The DMSO concentrations at the interface now surpass the previous saturation limit, and become identical to the concentration in the bulk water. We also observe that both DMSO and water appear to penetrate deeper into the ceramide membrane. These changes are consistent with the transition, as observed visually from the simulation trajectories (Fig. 9).

Area/lipid

The projected area/lipid as a function of DMSO concentration is shown in Fig. 12. At low concentrations (≤0.3 mol fraction DMSO), at which the bilayer is in the gel phase, there is only a small increase in the area/lipid compared to the system without DMSO. This minor change in the area/lipid in going from the pure system to those containing DMSO is probably due to some of the headgroup-headgroup or headgroup-water interactions being replaced by headgroup-DMSO interactions. Further, there appears to be no difference between the bilayer systems containing 0.1, 0.2, and 0.3 mol fraction DMSO, which is not surprising in light of the discussion above concerning the accumulation of DMSO at the interface, as the amount of DMSO at the interface is unchanged in these systems. At concentrations ≥0.4 mol fraction DMSO, the bilayer shows significant lateral expansion, as expected for the transition from a partially interdigitated gel phase to a liquid-crystalline phase with a higher degree of interdigitation.

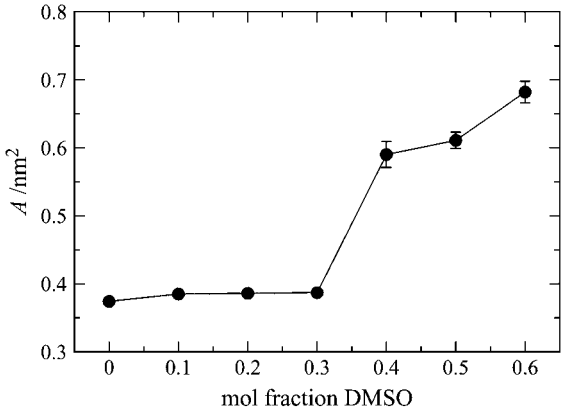

FIGURE 12 Area/lipid for the ceramide bilayer systems as a function of DMSO concentration.

Bilayer thickness

The bilayer thickness is another useful indicator of phase characterization. The thickness was calculated as the distance between the peaks of the ceramide headgroup density and is presented as a function of DMSO concentration in Fig. 13. It is essentially unchanged in the presence of low concentrations of DMSO but decreases by ~1.5 nm for the higher concentrations of DMSO corresponding to the transition to the liquid-crystalline phase. The change in the bilayer thickness is opposite to the change in the area/lipid, as expected if the average volume of the bilayer is to remain roughly constant. The observed increase of this volume by ~15% is due to the less optimal packing of the ceramides in the liquid-crystalline phase relative to the gel phase, and to the lateral swelling of the bilayer by DMSO molecules penetrating between and below the ceramide headgroups.

Lipid tail order

The lipid-tail-order parameters S_z for the ceramide hydrocarbon chains for the pure bilayer in the gel phase and bilayer

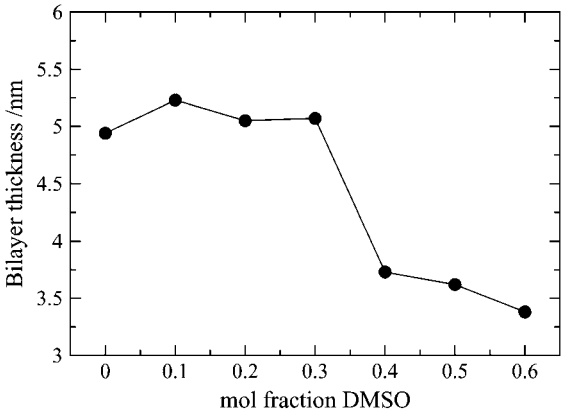

FIGURE 13 Thickness of the ceramide bilayer systems as a function of DMSO concentration.

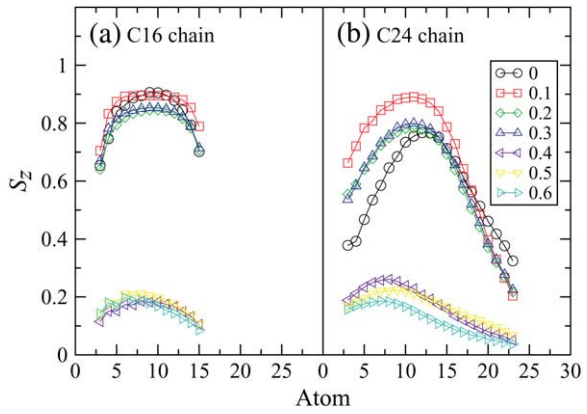

FIGURE 14 Lipid-tail-order parameters, S_z that indicate the alignment of the chain as a function of carbon number (indicated in Fig. 1) for the various ceramide bilayer systems containing different concentrations of DMSO.

systems containing DMSO are presented in Fig. 14. The order parameters fall into three groups corresponding to the pure ceramide bilayer, bilayer systems with 0.1−0.3 mol fraction DMSO (gel-phase structure), and systems with ≥0.4 mol fraction DMSO (liquid-crystalline phase). There is an increase in the tail order parameters for the long chain in going from the pure ceramide system to one containing 0.1 mol fraction DMSO. As discussed earlier, the ceramide gel phase shows extensive disorder of the alkyl groups close to the interface due to the partial retraction of the long-chain tails from the bilayer and to some lipids straddling others. This disorder vanishes in the presence of low concentrations of DMSO. Examination of the simulation trajectories shows that this is due to DMSO encouraging more of the ceramide molecules to adopt a hairpin conformation and minimizing the number of alkyl chains sticking out into the interface region. DMSO may bridge the gaps between ceramides, increasing the effective size of the headgroups and improving the hydrophobic shielding, so that the hairpin conformation becomes more stable. The change in ceramide conformation as 0.1 mol fraction DMSO is added to the bilayer is fully reversible, i.e., when the DMSO is removed from the system and replaced with water the ceramide molecules revert back to the conformations shown in Fig. 5, and the order-parameter plot returns to that given in Fig. 14 for the bilayer without DMSO. Increasing the DMSO concentration to 0.2 or 0.3 mol fraction slightly reduces the alignment of the tails, followed by a drastic drop for ≥0.4 mol fraction. That order parameters are low at these high concentrations suggests that the lipid tails are no longer straightened out, but have adopted coil-like conformations. This is confirmed by visual inspection of the membranes, which also reveals a very diffuse interface between the two leaflets of the bilayer.

Hydrogen bonding

The average number of ceramide-ceramide, ceramide-water, and ceramide-DMSO hydrogen bonds per ceramide molecule are given in Table 3. As stated earlier, in the pure ceramide system each ceramide molecule forms about three hydrogen bonds with its ceramide neighbors and hardly any with water. In systems containing low concentrations of DMSO, it appears that, on average, one of the ceramide-ceramide hydrogen bonds is replaced by a ceramide-DMSO hydrogen bond, whereas the ceramide-water hydrogen bonds have been almost eradicated. It is interesting to note that water preferentially forms hydrogen bonds with the carboxyl oxygen of the ceramide, whereas DMSO forms hydrogen bonds with the hydroxyl and amide groups of the ceramide, which suggests that DMSO and water compete for different positions on the ceramide headgroup. The DMSO accumulates at the interface, as it can form numerous strong hydrogen interactions with the ceramide headgroups, and this accumulation of DMSO at the interface shields the water from the ceramides and eradicates the ceramide-water hydrogen bonds. At the gel-to-liquid-crystal transition, a second ceramide-ceramide hydrogen bond is replaced by a ceramide-DMSO hydrogen bond, thereby considerably weakening the stability of the hydrogen-bonding network connecting the ceramides. The disruption of the ceramide-ceramide hydrogen-bond network by DMSO appears to be nonspecific, i.e., DMSO does not favor any one particular hydrogen-bond site on the ceramide headgroups.

TABLE 3 Average number of ceramide-water, ceramide-DMSO, and ceramide-ceramide hydrogen bonds per ceramide molecule in bilayer systems containing different concentrations of DMSO

DMSO (mol fraction)	Average number of hydrogen bonds per ceramide molecule		
	Ceramide-water	Ceramide-DMSO	Ceramide-ceramide
0.0	0.3	—	2.8
0.1	0.03	1.2	2.0
0.2	0.02	1.2	2.0
0.3	0.01	1.2	2.0
0.4	0.01	2.3	1.1
0.5	0.02	2.4	0.9
0.6	0.01	2.5	0.8

Elasticity

The area compressibility moduli are plotted as a function of DMSO concentration in Fig. 8. The area compressibility modulus for the pure system is higher than that of 0.1−0.3 mol fraction DMSO systems, which in turn are an order of magnitude higher than those of the 0.4−0.6 mol fraction DMSO systems. Therefore, the bilayers become increasingly more amenable to stretching (or compression) with increase in DMSO concentration. This behavior is probably a consequence of the DMSO molecules acting as spacers between the lipids and in so doing weakening the lateral forces, and as a result of DMSO shielding the ceramide tails from the water as the bilayer is stretched.

DISCUSSION

The objectives of this study were to develop and test a potential model for ceramide 2, to gain a molecular level understanding of the structural features and phase behavior of ceramide 2 bilayers as a function of temperature, and then to investigate the interaction of DMSO with the gel-phase structure of the ceramide. The DMSO interaction with the ceramide bilayers is of interest in understanding how DMSO, and other short chain amphiphilic molecules such as alcohols, enhance the permeability of skin. Although we acknowledge that the skin lipids are heterogeneous in composition and that their organization is complex, it is well accepted that the primary properties of the skin lipids are governed by the constituent ceramides. In view of this, we expect bilayers of ceramide 2 (the predominant ceramide in skin lipids) to yield characteristics and behavior that are fundamental to skin lipids. Consequently, how DMSO interacts with ceramide 2 bilayers may also be an important feature of the action of DMSO in enhancing permeability in real skin.

On the whole, the ceramide potential model employed reproduces both the phase behavior and the few known structural parameters of ceramide 2 bilayers with reasonable accuracy. The model yields a hexagonal gel-phase bilayer structure at 283 and 323 K, and a liquid-crystalline bilayer at 363 K, which are consistent with experimental observations of a hexagonal gel-phase structure below ~360 K and a fluid structure above this temperature (15,22). Experimentally, ceramide 2 can also exhibit an orthorhombic gel phase below 333 K (15), which was not observed in the simulations. This deficiency may be attributed to the potential model but could also result from kinetic factors. In addition to the phase behavior, the other available experimental data are the area/lipid for the gel-phase monolayers and the bilayer thickness in the crystalline phase. The ceramide potential model yields an area/lipid of 0.374 nm^2 for the gel phase, which is remarkably close to the experimental value of 0.378 nm^2 (27). The bilayer thickness for the gel phase is ~4.9 nm, which compares favorably with that in the crystal structure (hairpin conformation), namely, 5.2 nm (54).

Structurally, the ceramide 2 bilayers reveal some unique features that result from the inherent flexibility of the ceramide 2 molecule, the asymmetry in its tail lengths, and the strong ceramide-ceramide hydrogen-bonding network. Ceramides have the ability to adopt a number of conformations, including the classic hairpin and extended conformations where the molecule is essentially linear or obtuse-V-shaped (17,54,59,60). In contrast, phospholipids such as DPPC tend to restrict themselves to the classic hairpin conformation. This conformational flexibility of ceramides is a consequence of their small headgroup. In the bilayer structures, the ceramide 2 molecules appear to exploit this flexibility in a bid to pack their asymmetric tails in a commensurate way. The asymmetric tails do not interdigitate in a coherent manner, and some of the molecules readily expose their alkyl groups at the ceramide-water interface to reduce the tail-end packing frustration at the bilayer core. Thus, the molecules retract their tails or straddle over neighbors and in so doing expose some of the alkyl groups at the ceramide-water interface. In some instances, the molecules present an entire tail tangentially at the ceramide-water interface. The free energy penalty here may not be as high as might be perceived, as the poor hydrophobic shielding by the small headgroups and the resulting high density of the alkyl groups exposed at the interface are likely to make the interface more hospitable to a hydrocarbon tail. The overall result is that the interface takes on a more hydrophobic character and is sharp, with little or no water penetration, which explains the low water permeability of the stratum corneum. For a given phase, the ceramide bilayers are relatively less compressible (have a high area compressibility modulus) than corresponding phospholipid bilayers. The strong rigidity of the bilayers appears to stem from the strong lateral hydrogen bonding between the ceramide molecules, with each molecule involved in about three hydrogen bonds on average, and the high interfacial free energy due to the hydrophobic nature of the interface.

Considering the interaction of DMSO with the gel phase of ceramide 2, we observe that low concentrations of DMSO suffice to make the bilayer less rigid, whereas high concentrations induce the gel-phase structure to undergo a phase transition to the liquid-crystalline phase. At the molecular level, the DMSO molecules tend to accumulate at the interface, where they displace the water molecules. This is not surprising given that the DMSO molecule is amphiphilic. At high concentrations, the DMSO molecules integrate into the headgroup region, becoming involved in hydrogen bonding with the ceramide headgroups at the expense of the ceramide-ceramide hydrogen bonds. This disruption of the ceramide-ceramide hydrogen bonds enables the DMSO molecules to penetrate a little deeper and to effectively act as spacers. The lateral expansion of the bilayer destabilizes the lipid-tail packing, which results in the phase transition to the liquid crystalline phase. The resulting liquid-crystalline phase is characterized by a reduced bilayer thickness, a high degree of disorder of the lipid tails, and a low area compressibility modulus.

The observation that DMSO induces a gel-to-liquid-crystalline phase transition in the ceramide bilayers is consistent with experimental data that DMSO fluidizes the stratum corneum lipids at high concentrations (32,33). Furthermore, it is only at high concentrations ($\geq$0.26% mol fraction) that DMSO exerts its permeability enhancement effect on the stratum corneum in any significant way (4,33,61). The fact that in the simulated ceramide 2 bilayers only high concentrations of DMSO ($\geq$0.4 mol fraction) are able to induce the gel-to-liquid-crystalline phase transition in the ceramide 2 bilayers, whereas a reverse transition is observed when lowering the DMSO concentration to 0.3, is consistent with these experimental observations. In terms of permeability,

the liquid-crystalline bilayer is expected to offer a significantly lower resistance to a permeating molecule in comparison with the gel-phase bilayer. The hydrocarbon region of a liquid-crystalline phase is expected to enable a higher rate of diffusion and offer a markedly lower free-energy barrier to a permeating molecule. The liquid-crystalline bilayer, having a lower thickness, will also present a shorter diffusion path length to the permeating molecule. On the basis of these results and the postulate that the properties of the stratum corneum are largely determined by the ceramide constituents, we propose that DMSO—at sufficiently high concentrations—enhances the permeability of the stratum corneum by inducing a phase transition of the lipids from their natural gel-phase state to the more permeable liquid-crystalline structure.

How DMSO interacts with the phospholipid DPPC has been investigated previously, albeit only for the liquid-crystalline phase and employing coarse-grained models (41). These studies suggest that DMSO makes the phospholipid bilayers less rigid (the area compressibility and bending moduli are lowered), and at high concentrations can induce water pores in the membrane. At the molecular level, the interaction of DMSO with the phospholipid bilayer is essentially similar to that with the ceramide 2 bilayer in that the DMSO molecules accumulate about the headgroup region, where they act as spacers and reduce the lipid-lipid interaction and also serve to shield the hydrocarbon tails. For the ceramide bilayers the bending rigidity could not be determined, because the bilayer was too rigid to sustain appreciable thermal undulations, but we expect that it will be lowered by DMSO. Both of these changes in the mechanical properties of the bilayers are essential in enhancing the possibility of pore formation. In view of this, the possibility that DMSO could induce pores in the ceramide liquid-crystalline bilayers exists, but the probability is expected to be low due to the stronger lipid-lipid interaction for ceramides compared with phospholipids.

In conclusion, we have carried out simulations of ceramide 2 bilayers in the gel phase with different concentrations of DMSO (0.0−0.6 mol fraction). DMSO at high concentrations ($\geq$0.4 mol fraction) induces the gel-phase structure to undergo a transition to the liquid-crystalline phase. The origin of this transition appears to be the accumulation of DMSO molecules at the headgroup region, where the molecules integrate, making hydrogen bonds with the lipid headgroups at the expense of the ceramide-ceramide hydrogen bonding. The weakening of the lateral forces and the ensuing expansion in the lipid area causes destabilization of the lipid tail packing resulting in the phase transition to the liquid-crystalline structure. The liquid-crystalline phase of ceramides is expected to be markedly more permeable to solutes than the gel-phase structure. These results are consistent with the experimental evidence that high concentrations of DMSO both fluidize the stratum corneum lipids and enhance their permeability.

Rebecca Notman is grateful to the Engineering and Physical Sciences Research Council and Unilever Research for the provision of an Industrial CASE studentship. The authors acknowledge SoftComp European Union Network of Excellence for providing the opportunity and financial support to R.N. to perform part of this work at the University of Twente (Eurothesis Program).

REFERENCES

1. Elias, P. M. 1983. Epidermal lipids, barrier function, and desquamation. *J. Invest. Dermatol.* 80(Suppl. 6):44–49.
2. Williams, A. C. 2003. Theoretical aspects of transdermal drug delivery. *In* Transdermal and Topical Drug Delivery. T. K. Ghosh, W. Pfister, and S. I. Yum, editors. Pharmaceutical Press: From Theory to Clinical Practice, London. 27–49.
3. Barry, B. W. 1983. Dermatological Formulations: Percutaneous Absoprtion. Informa Healthcare, London.
4. Williams, A. C., and B. W. Barry. 2004. Penetration enhancers. *Adv. Drug Del. Rev.* 56:603–618.
5. Williams, M. L., and P. M. Elias. 1987. The extracellular-matrix of stratum-corneum: role of lipids in normal and pathological function. *CRC Critical Reviews in Therapeutic Drug Carrier Systems.* 3:95–122.
6. Wertz, P. W., and D. T. Downing. 1996. The nature of the epidermal barrier: biochemical aspects. *Adv. Drug Del. Rev.* 18:283–294.
7. Bouwstra, J. A., F. E. R. Dubbelaar, G. S. Gooris, and M. Ponec. 2000. The lipid organisation in the skin barrier. *Acta Derm. Venereol.* 80(Suppl. 208):23–30.
8. Bouwstra, J. A., G. S. Gooris, M. A. Salomons-de Vries, J. A. van der Spek, and W. Bras. 1992. Structure of human stratum corneum as a function of temperature and hydration: a wide-angle X-ray diffraction study. *Int. J. Pharm.* 84:205–216.
9. Pilgram, G. S. K., A. M. Engelsma-van Pelt, J. A. Bouwstra, and H. K. Koerten. 1999. Electron diffraction provides new information on human stratum corneum lipid organization studied in relation to depth and temperature. *J. Invest. Dermatol.* 113:403–409.
10. Bommannan, D., R. O. Potts, and R. H. Guy. 1990. Examination of stratum corneum barrier function in vivo by infrared spectroscopy. *J. Invest. Dermatol.* 95:403–408.
11. Ongpipattanakul, B., M. L. Francoeur, and R. O. Potts. 1994. Polymorphism in stratum corneum lipids. *Biochim. Biophys. Acta.* 1190: 115–122.
12. Hauser, J. M. L., B. M. Buehrer, and R. M. Bell. 1994. Role of ceramide in mitogenesis induced by exogenous sphingoid bases. *J. Biol. Chem.* 269:6803–6809.
13. Perry, D. K., and Y. A. Hannun. 1998. The role of ceramide in cell signaling. *Biochim. Biophys. Acta.* 1436:233–243.
14. Kronke, M. 1999. Biophysics of ceramide signaling: interaction with proteins and phase transition of membranes. *Chem. Phys. Lipids.* 101: 109–121.
15. Moore, D. J., M. E. Rerek, and R. Mendelsohn. 1997. FTIR spectroscopy studies of the conformational order and phase behavior of ceramides. *J. Phys. Chem. B.* 101:8933–8940.
16. Moore, D. J., M. E. Rerek, and R. Mendelsohn. 1997. Lipid domains and orthorhombic phases in model stratum corneum: evidence from Fourier transform infrared spectroscopy studies. *Biochem. Biophys. Res. Commun.* 231:797–801.
17. Pascher, I. 1976. Molecular arrangements in sphingolipids: conformation and hydrogen bonding of ceramide and their implication on membrane stability and permeability. *Biochim. Biophys. Acta.* 455: 433–451.
18. Moore, D. J., M. E. Rerek, and R. Mendelsohn. 1999. Role of ceramides 2 and 5 in the structure of the stratum corneum lipid barrier. *Int. J. Cosmet. Sci.* 21:353–368.
19. Moore, D. J., and M. E. Rerek. 2000. Insights into the molecular organization of lipids in the skin barrier from infrared spectroscopy

studies of stratum corneum lipid models. *Acta Derm. Venereol.* 80(Suppl. 208):16–22.

20. Carrer, D. C., S. Schreier, M. Patrito, and B. Maggio. 2006. Effects of a short-chain ceramide on bilayer domain formation, thickness, and chain mobililty: DMPC and asymmetric ceramide mixtures. *Biophys. J.* 90: 2394–2403.
21. Shah, J., J. M. Atienza, R. I. Duclos, A. V. Rawlings, Z. Dong, and G. G. Shipley. 1995. Structual and thermotropic properties of synthetic C16:0 (palmitoyl) ceramide: effect of hydration. *J. Lipid Res.* 36:1936–1944.
22. Shah, J., J. M. Atienza, A. V. Rawlings, and G. G. Shipley. 1995. Physical properties of ceramides: effect of fatty acid hydroxylation. *J. Lipid Res.* 36:1945–1955.
23. Rerek, M. E., H.-C. Chen, B. Markovic, D. Van Wyck, P. Garidel, R. Mendelsohn, and D. J. Moore. 2001. Phytosphingosine and sphingosine ceramide headgroup hydrogen bonding: structural insights through thermotropic hydrogen/deuterium exchange. *J. Phys. Chem. B.* 105: 9355–9362.
24. de Jager, M. W., G. S. Gooris, I. P. Dolbnya, W. Bras, M. Ponec, and J. A. Bouwstra. 2003. The phase behaviour of skin lipid mixtures based on synthetic ceramides. *Chem. Phys. Lipids.* 124:123–134.
25. Sot, J., F. J. Aranda, M.-I. Collado, F. M. Goni, and A. Alonso. 2005. Different effects of long- and short-chain ceramides on the gel-fluid and lamellar-hexagonal transitions of phospholipids: a calorimetric, NMR, and x-ray diffraction study. *Biophys. J.* 88:3368–3380.
26. Scheffer, L., I. Solomonov, M. J. Weygand, K. Kjaer, L. Leiserowitz, and L. Addadi. 2005. Structure of cholesterol/ceramide monolayer mixtures: implications to the molecular organization of lipid rafts. *Biophys. J.* 88:3381–3391.
27. Brockman, H. L., M. M. Momsen, R. E. Brown, L. He, J. Chun, H.-S. Byun, and R. Bittman. 2004. The 4,5-double bond of ceramide regulates its dipole potential, elastic properties, and packing behavior. *Biophys. J.* 87:1722–1731.
28. Walker, R. B., and E. W. Smith. 1996. The role of percutaneous penetration enhancers. *Adv. Drug Del. Rev.* 18:295–301.
29. Hadgraft, J. 1999. Passive enhancement strategies in topical and transdermal drug delivery. *Int. J. Pharm.* 184:1–6.
30. Karande, P., A. Jain, and S. Mitragotri. 2004. Discovery of transdermal penetration enhancers by high-throughput screening. *Nat. Biotechnol.* 22:192–197.
31. Smith, E. W., and H. I. Maiback. 2005. Percutaneous Enhancers, 2nd ed. CRC Press, Boca Raton, FL.
32. Barry, B. W. 1987. Mode of action of penetration enhancers in human skin. *J. Controlled Release.* 6:85–97.
33. Anigbogu, A. N. C., A. C. Williams, B. W. Barry, and H. G. M. Edwards. 1995. Fourier transform Raman spectroscopy of interactions between the penetration enhancer dimethyl sulfoxide and human stratum corneum. *Int. J. Pharm.* 125:265–282.
34. Oertel, R. P. 1977. Protein conformational changes induced in human stratum corneum by organic sulfoxides: an infrared spectroscopic investigation. *Biopolymers.* 16:2329–2345.
35. Anchordoguy, T. J., J. F. Carpenter, J. H. Crowe, and L. M. Crowe. 1992. Temperature-dependent perturbation of phospholipid bilayers by dimethylsulfoxide. *Biochim. Biophys. Acta.* 1104:117–122.
36. Yu, Z. W., and P. J. Quinn. 1998. The modulation of membrane structure and stability by dimethyl sulphoxide (review). *Mol. Membr. Biol.* 15:59–68.
37. Rall, W. F., and G. M. Fahy. 1985. Ice-free cryopreservation of mouse embryos at −196°C by vitrification. *Nature.* 313:573–575.
38. Kasai, M. 2002. Advances in the cryopreservation of mammalian oocytes and embryos: development of ultrarapid vitrification. *Reprod. Med. Biol.* 1:1–9.
39. Smondyrev, A. M., and M. L. Berkowitz. 1999. Molecular dynamics simulation of DPPC bilayer in DMSO. *Biophys. J.* 76:2472–2478.
40. Sum, A. K., and J. J. de Pablo. 2003. Molecular simulation study on the influence of dimethylsulfoxide on the structure of phospholipid bilayers. *Biophys. J.* 85:3636–3645.
41. Notman, R., M. Noro, B. O'Malley, and J. Anwar. 2006. Molecular basis for dimethylsulfoxide (DMSO) action on lipid membranes. *J. Am. Chem. Soc.* 128:13982–13983.
42. Höltje, M., T. Forster, B. Brandt, T. Engels, W. von Rybinski, and H.-D. Holtje. 2001. Molecular dynamics simulations of stratum corneum lipid models: fatty acids and cholesterol. *Biochim. Biophys. Acta.* 1511:156–167.
43. Anishkin, A., S. Sukharev, and M. Colombini. 2006. Searching for the molecular arrangement of transmembrane ceramide channels. *Biophys. J.* 90:2414–2426.
44. Pandit, S. A., and H. L. Scott. 2006. Molecular-dynamics simulation of a ceramide bilayer. *J. Chem. Phys.* 124:014708.
45. Berger, O., O. Edholm, and F. Jahnig. 1997. Molecular dynamics simulations of a fluid bilayer of dipalmitoylphosphatidylcholine at full hydration, constant pressure, and constant temperature. *Biophys. J.* 72:2002–2013.
46. Mombelli, E., R. Morris, W. Taylor, and F. Fraternali. 2003. Hydrogen-bonding propensities of sphingomyelin in solution and in a bilayer assembly: a molecular dynamics study. *Biophys. J.* 84:1507–1517.
47. Berendsen, H. J. C., J. P. M. Postma, W. F. van Gunsteren, and W. F. Hermans. 1981. Interaction models for water in relation to protein hydration. *In* Intermolecular Forces. B. Pullman, editor. D. Reidel Publishing, Dordrecht, The Netherlands. 331–342.
48. Bordat, P., J. Sacristan, D. Reith, S. Girard, A. Glattli, and F. Muller-Plathe. 2003. An improved dimethyl sulfoxide force field for molecular dynamics simulations. *Chem. Phys. Lett.* 374:201–205.
49. Lindahl, E., B. Hess, and D. van der Spoel. 2001. GROMACS 3.0: A package for molecular simulation and trajectory analysis. *J. Mol. Model.* 7:306–317.
50. Ryckaert, J. P., G. Ciccotti, and H. J. C. Berendsen. 1977. Numerical integration of the equations of motion for a system with constraints: molecular dynamics of *n*-alkanes. *J. Comput. Phys.* 23:327–341.
51. Patra, M., M. Karttunen, M. T. Hyvonen, E. Falck, P. Lindqvist, and I. Vattulainen. 2003. Molecular dynamics simulations of lipid bilayers: major artifacts due to truncating electrostatic interactions. *Biophys. J.* 84:3636–3645.
52. Wohlert, J., and O. Edholm. 2004. The range and shielding of dipole-dipole interactions in phospholipid bilayers. *Biophys. J.* 87:2433–2445.
53. Chen, H.-C., R. Mendelsohn, M. E. Rerek, and D. J. Moore. 2000. Fourier transform infrared spectroscopy and differential scanning calorimetry studies of fatty acid homogeneous ceramide 2. *Biochim. Biophys. Acta.* 1468:293–303.
54. Dahlen, B., and I. Pascher. 1979. Molecular arrangements in sphingolipids. Thermotropic phase behaviour of tetracosanoylphytosphingosine. *Chem. Phys. Lipids.* 24:119–133.
55. Van der Spoel, D., E. Lindahl, B. Hess, A. R. van Buuren, E. Apol, P. J. Meulenhoff, D. P. Tieleman, A. L. T. M. Sijbers, K. A. Feenstra, R. van Drunen, and H. J. C. Berendsen. 2004. Gromacs User Manual version 3.2. http://www.gromacs.org/.
56. Herce, H. D., and A. E. Garcia. 2006. Correction of apparent finite size effects in the area per lipid of lipid membrane simulations. *J. Chem. Phys.* 125:224711.
57. Rand, R. P., and V. A. Parsegian. 1989. Hydration forces between phospholipid bilayers. *Biochim. Biophys. Acta.* 988:351–376.
58. Chiu, S. W., S. Vasudevan, E. Jakobsson, R. J. Mashl, and H. L. Scott. 2003. Structure of sphingomyelin bilayers: a simulation study. *Biophys. J.* 85:3624–3635.
59. Dahlen, B., and I. Pascher. 1972. Molecular arrangements in sphingolipids. Crystal structure of N-tetracosanoylphytosphingosine. *Acta Crystallogr., Sect. B: Struct. Crystallogr. Cryst. Chem.* 28:2396–2404.
60. Pascher, I., and S. Sundell. 1992. Molecular arrangements in sphingolipids: crystal structure of the ceramide N-(2D,3D-dihydroxyoctadecanoyl)-phytosphingosine. *Chem. Phys. Lipids.* 61:79–86.
61. Kligman, A. M. 1965. Topical pharmacology and toxicology of dimethyl sulphoxide. 1. *JAMA.* 193:796–804.